Cross Metathesis on Olefin-Terminated Monolayers on Si(111) Using the Grubbs' Catalyst

Samrat Dutta,[†] Mathew Perring,[†] Stephen Barrett,[†] Michael Mitchell,[‡] Paul J. A. Kenis,[‡] and Ned B. Bowden*,[†]

Department of Chemistry, University of Iowa, 423K Chemistry Building, Iowa City, Iowa 52242, and Department of Chemical and Biomolecular Engineering, University of Illinois at Urbana-Champaign, 600 South Mathews Avenue, Urbana, Illinois 61801

Received November 29, 2005. In Final Form: December 8, 2005

This paper reports the functionalization and patterning of olefin-terminated monolayers on Si(111) through cross metathesis. A simple, one-step synthesis of a diolefin—CH_2═$CH(CH_2)_9O(CH_2)_9CH$═CH_2—was developed from commercially available starting materials. Mixed partially olefin-terminated monolayers of this novel diolefin and 1-octadecene on hydrogen-terminated Si(111) were obtained. The olefins are raised above the rest of the monolayer and thus sterically accessible for further functionalization. Olefin-terminated monolayers were reacted with the Grubbs' first generation catalyst and olefins in solution that were terminated with fluorines, carboxylic acids, alcohols, aldehydes, and alkyl bromides. Characterization of these monolayers using X-ray photoelectron spectroscopy and horizontal attenuated total reflection infrared spectroscopy demonstrated that olefins on the surface had reacted via cross metathesis to expose fluorines, carboxylic acids, aldehydes, alcohols, and bromides. Through calibration experiments, we demonstrated a simple 1:1 correspondence between the ratio of olefins in solution used in the assembly and the final composition of the mixed monolayers. Finally, these monolayers on silicon were patterned on the micrometer-size scale by soft lithography using microfluidic channels patterned into poly(dimethylsiloxane) (PDMS) stamps. Micrometer-wide lines of polymer brushes were synthesized on these monolayers and characterized by scanning electron microscopy. In addition, olefin-terminated monolayers were patterned into micrometer-sized lines exposing carboxylic acids by cross metathesis with olefins in solution. This method of patterning is broadly applicable and can find applications in a variety of fields including the development of biosensors and nanoelectronics.

Introduction

The field of monolayers on silicon is growing rapidly as new, mild methods for their assembly have been recently reported.[1−6] Self-assembled monolayers (SAMs) on silicon are an important area of research as they combine the selectivity of organic chemistry with the terrific electronic properties of silicon. For instance, new sensors that expose DNA, proteins, carbohydrates, porphyrins, or other biologically relevant functional groups on the surface of monolayers on silicon have been reported.[6−8] These sensors offer new possibilities to exploit the opportunities of combining biotechnology with silicon technology and will open up new avenues in science and technology.

Despite these advances, methods to assemble monolayers on silicon are intolerant of most functional groups or require multiple gram quantities of starting materials that make them impractical for the synthesis and assembly of complex, expensive molecules. Methods to assemble monolayers on silicon begin with hydrogen-terminated Si(111); this surface is unstable and readily oxidizes to form a thin layer of SiO_x on the surface.[9,10] Although crystalline monolayers on silicon protect it from oxidation, the assembly is slow such that side reactions between hydrogen-terminated Si-(111) and most functional groups limits what can be displayed. The most successful approach around this problem is to first

* Corresponding author. E-mail: ned-bowden@uiowa.edu.
[†] University of Iowa.
[‡] University of Illinois.

(1) Wayner, D. D. M.; Wolkow, R. A. *J. Chem. Soc., Perkin Trans.* **2002**, *2*, 23−34. Li, X.-M.; Huskens, J.; Reinhoudt, D. N. *J. Mater. Chem.* **2004**, *14*, 2954−2971. Sieval, A. B.; Vleeming, V.; Zuilhof, H.; Sudholter, E. J. R. *Langmuir* **1999**, *15*, 8288−8291. Zhu, X.-Y.; Jun, Y.; Staarup, D. R.; Major, R. C.; Danielson, S.; Boiadjiev, V.; Gladfelter, W. L.; Bunker, B. C.; Guo, A. *Langmuir* **2001**, *17*, 7798−7803. Bergerson, W. F.; Mulder, J. A.; Hsung, R. P.; Zhu, X.-Y. *J. Am. Chem. Soc.* **1999**, *121*, 454−455. Boukherroub, R.; Wayner, D. D. M. *J. Am. Chem. Soc.* **1999**, *121*, 11513−11515. Kim, N. Y.; Laibinis, P. E. *J. Am. Chem. Soc.* **1997**, *199*, 22297-2298. Kim, N. Y.; Laibinis, P. E. *J. Am. Chem. Soc.* **1998**, *120*, 4516−4517. Zhang, L.; Wesley, K.; Jiang, S. *Langmuir* **2001**, *17*, 6275−6281. Uosaki, K.; Quayum, M. E.; Nihonyanagi, S.; Kondo, T. *Langmuir* **2004**, *20*, 1207−1212. Bansal, A.; Li, X.; Lauermann, I.; Lewis, N. S. *J. Am. Chem. Soc.* **1996**, *118*, 7225−7226. Bansal, A.; Li, X.; Yi, S. I.; Weinberg, W. H.; Lewis, N. S. *J. Phys. Chem. B* **2001**, *105*, 10266−10277. Sung, M. M.; Kluth, G. J.; Yauw, O. W.; Maboudian, R. *Langmuir* **1997**, *13*, 6164−6168. Buriak, J. M. *Chem. Commun.* **1999**, *12*, 1051−1060. Buriak, J. M.; Allen, M. J. *J. Am. Chem. Soc.* **1998**, *120*, 1339−1340. Liu, Y.-J.; Navasero, N. M.; Yu, H.-Z. *Langmuir* **2004**, *20*, 4039−4050. Sun, Q.-Y.; De Smet, L. C. P. M.; Van Lagen, B.; Giesbers, M.; Thuene, P. C.; Van Engelenburg, J.; De Wolf, F. A.; Zuilhof, H.; Sudhoelter, E. J. R. *J. Am. Chem. Soc.* **2005**, *127*, 2514−2523. Sun, Q.-Y.; de Smet, L. C. P. M.; van Lagen, B.; Wright, A.; Zuilhof, H.; Sudhoelter, E. J. R. *Angew. Chem., Int. Ed.* **2004**, *43*, 1352−1355.

(2) Li, Y. J.; Tero, R.; Nagasawa, T.; Ngata, T.; Urisu, T. *Appl. Surf. Sci.* **2004**, *238*, 238−241. Boukherroub, R.; Morin, S.; Bensebaa, F.; Wayner, D. D. M. *Langmuir* **1999**, *15*, 3831−3835.

(3) Sieval, A. B.; Demirel, A. L.; Nissink, J. W. M.; Linford, M. R.; van der Maas, J. H.; de Jeu, W. H.; Zuilhof, H.; Sudholter, E. J. R. *Langmuir* **1998**, *14*, 1759−1768.

(4) Sieval, A. B.; Linke, R.; Zuilhof, H.; Sudhölter, E. J. R. *Adv. Mater.* **2000**, *12*, 1457−1460.

(5) Linford, M. R.; Chidsey, C. E. D. *Langmuir* **2002**, *18*, 6217−6221. Linford, M. R.; Fenter, P.; Eisenberger, P. M.; Chidsey, C. E. D. *J. Am. Chem. Soc.* **1995**, *117*, 3145−3155.

(6) de Smet, L. C. P. M.; Stork, G. A.; Hurenkamp, G. H. F.; Sun, Q.-Y.; Topal, H.; Vronen, P. J. E.; Sieval, A. B.; Wright, A.; Visser, G. M.; Zuilhof, H.; Sudhoelter, E. J. R. *J. Am. Chem. Soc.* **2003**, *125*, 13916−13917. de Smet, L. C. P. M.; Pukin, A. V.; Stork, G. A.; Ric de Vos, C. H.; Visser, G. M.; Zuilhof, H.; Sudhoelter, E. J. R. *Carbohydr. Res.* **2004**, *339*, 2599−2605. Ara, M.; Tada, H. *Appl. Phys. Lett.* **2003**, *83*, 578−580. Lasseter, T. L.; Clare, B. H.; Abbott, N. L.; Hamers, R. S. *J. Am. Chem. Soc.* **2004**, *126*, 10220−10221. Liao, W.; Wei, F.; Qian, M. X.; Zhao, X. S. *Sens. Actuators, B* **2004**, *B101*, 361−367.

(7) Strother, T.; Cai, W.; Zhao, X.; Hamers, R. J.; Smith, L. M. *J. Am. Chem. Soc.* **2000**, *122*, 1205−1209. Voicu, R.; Boukherroub, R.; Bartzoka, V.; Ward, T.; Wojtyk, J. T. C.; Wayner, D. D. M. *Langmuir* **2004**, *20*, 11713−11720.

(8) Pike, A. R.; Lie, L. H.; Eagling, R. A.; Ryder, L. C.; Patole, S. N.; Connolly, B. A.; Horrocks, B. R.; Houlton, A. *Angew. Chem., Int. Ed.* **2002**, *41*, 615−617.

(9) Burrows, V. A.; Chabal, Y. J.; Higashi, G. S.; Raghavachari, K.; Christman, S. B. *Appl. Phys. Lett.* **1988**, *53*, 998−1000. Wade, C. P.; Chidsey, C. E. D. *Appl. Phys. Lett.* **1997**, *71*, 1679−1681.

(10) Higashi, G. S.; Chabal, Y. J.; Trucks, G. W.; Raghavachari, K. *Appl. Phys. Lett.* **1990**, *56*, 656−658.

10.1021/la0532196 CCC: $33.50
Published on Web 01/17/2006

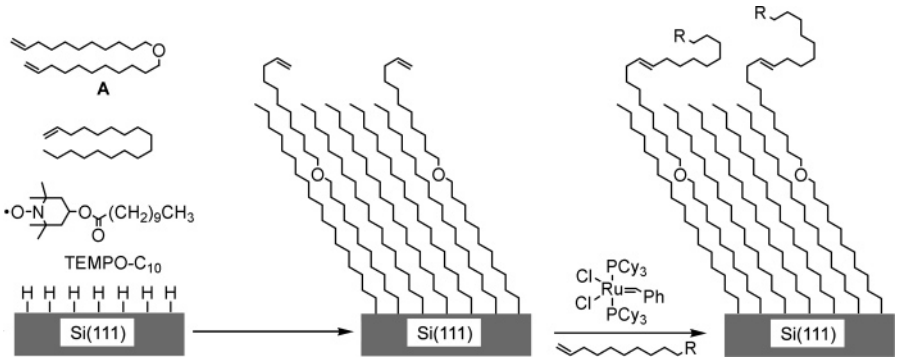

Figure 1. Our method to assemble and functionalize olefin-terminated monolayers by cross metathesis. A silicon wafer with a native layer of SiO_x was cleaned and then placed in Ar-purged 40% H_4NF for 30 min to form a hydrogen-terminated Si(111) surface. The wafer was immediately immersed in a solution of **A**, 1-octadecene, and trace amounts of TEMPO-C_{10} for 24 h. Cross metathesis between olefin-terminated monolayers and olefins with different "R" groups including carboxylic acids, alcohols, bromides, and aldehydes was catalyzed by the ruthenium-based Grubbs' first generation catalyst.

Scheme 1. Example of Cross Metathesis between Two Olefins and Catalyzed by the Grubbs' First Generation Catalyst

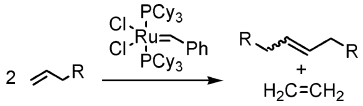

assemble an ordered monolayer and functionalize it in a second step.[1−6] In this paper we report a new, versatile approach that uses cross metathesis via the Grubbs' first generation catalyst to functionalize olefin-terminated monolayers on silicon with a wide variety of functional groups.

We and others recently reported mild methods to assemble well-ordered monolayers on Si(111) that can extend the range of functional groups displayed on its surface.[1−6,11,12] Monolayers on Si(111) that display esters, amides, alcohols, acids, alkyl halides, and acid chlorides have been assembled and characterized. These monolayers are useful as they can be functionalized in subsequent steps, but important questions remain about their stabilities or whether these monolayers can be assembled over large areas. For instance, reports on acid-terminated monolayers demonstrated that they had limited stabilities in aqueous solvents or their stabilities were not reported.[2,7,11,13] Monolayers terminated with alkyl halides or acid chlorides were assembled by scribing silicon and yielded a monolayer covering a fraction of the area of a silicon wafer.[3,14] The field of monolayers on silicon would benefit greatly from more mild methods to assemble functional monolayers that protect the surface from oxidation.

We wished to assemble olefin-terminated monolayers as Si(111)−H is tolerant of this functional group and these olefins provide a useful functional group for further functionalization through cross metathesis (Scheme 1).[11,12] Cross metathesis is a simple reaction, the reaction between two terminal olefins results in the formation of a double bond and the release of ethylene.[15] The release of ethylene can be used to drive this reaction to quantitative conversions. We choose to use the Grubbs' first generation catalyst as it is less sensitive to functional groups than those based on Ti, Mo, and W; it catalyzes cross metathesis reactions at low catalyst loadings; and it is over four times less expensive than the Grubbs' second generation catalyst.[15] This catalyst has been used to carry out cross metathesis reactions between proteins, carbohydrates, crown ethers, and numerous small molecules displaying acids, halides, alcohols, esters, amides, and amines.[15]

We and others have reported metathesis reactions on monolayers on gold, silicon dioxide, or silicon.[11,16] In most of these examples the Grubbs' catalyst was reacted with strained, cyclic olefins on a monolayer and used to grow polymer brushes from surfaces by ring opening metathesis polymerization (ROMP). In one example, crystalline monolayers of $HS(CH_2)_9CH{=}CH_2$ were assembled on gold and were reacted by cross metathesis with the Grubbs' second generation catalyst and olefins in solution.[17] These monolayers were not patterned nor were the monolayers designed such that the olefins would be sterically accessible to react with the Grubbs' catalyst.

In previous work we showed that monolayers assembled from 1-octadecene and trace amounts of TEMPO-C_{10} (see Figure 1 for the structure of TEMPO-C_{10}) were stable and protected the silicon surface from oxidation upon exposure to ambient conditions for over 2 months, water at room temperature for over 20 days, chloroform at room temperature for over 14 days, and

(11) Perring, M.; Dutta, S.; Arafat, S.; Mitchell, M.; Kenis, P. J. A.; Bowden, N. B. *Langmuir* **2005**, *21*, 10537−10544.

(12) Arafat, S. N.; Dutta, S.; Perring, M.; Mitchell, M.; Kenis, P. J. A.; Bowden, N. B. *Chem. Commun.* **2005**, *25*, 3198−3200.

(13) Cattaruzza, F.; Cricenti, A.; Flamini, A.; Girasole, M.; Longo, G.; Mezzi, A.; Prosperi, T. *J. Mater. Chem.* **2004**, *14*, 1461−1468. Cai, W.; Peck, J. R.; van der Weide, D. W.; Hamers, R. J. *Biosens. Bioelectron.* **2004**, *19*, 1013−1019.

(14) Jiang, G.; Niederhauser, T. L.; Davis, S. D.; Lua, Y.-Y.; Cannon, B. R.; Dorff, M. J.; Howell, L. L.; Magleby, S. P.; Linford, M. R. *Colloids Surf., A* **2003**, *226*, 9−16. Lua, Y.-Y.; Fillmore, W. J. J.; Linford, M. R. *Appl. Surf. Sci.* **2004**, *231*−*232*, 323−327. Niederhauser, T. L.; Lua, Y.-Y.; Jiang, G.; Davis, S. D.; Matheson, R.; Hess, D. A.; Mowat, I. A.; Linford, M. R. *Angew. Chem., Int. Ed.* **2002**, *41*, 2353−2356. Wagner, P.; Nock, S.; Spudich, J. A.; Volkmuth, W. D.; Chu, S.; Cicero, R. L.; Wade, C. P.; Linford, M. R.; Chidsey, C. E. D. *J. Struct. Biol.* **1997**, *119*, 189−201.

(15) Liu, Z.; Rainier, J. D. *Org. Lett.* **2005**, *7*, 131−133. Bielawski, C. W.; Grubbs, R. H. *Macromolecules* **2001**, *34*, 8838−8840. Sanford, M. S.; Love, J. A.; Grubbs, R. H. *J. Am. Chem. Soc.* **2001**, *123*, 6543−6554. Schwab, P.; Grubbs, R. H.; Ziller, J. W. *J. Am. Chem. Soc.* **1996**, *118*, 100−110. Trnka, T. M.; Grubbs, R. H. *Acc. Chem. Res.* **2001**, *34*, 18−29. Blackwell, H. E.; O'Leary, D. J.; Chatterjee, A. K.; Washenfelder, R. A.; Bussmann, D. A.; Grubbs, R. H. *J. Am. Chem. Soc.* **2000**, *122*, 58−71. Sanford, M. S.; Henling, L. M.; Day, M. W.; Grubbs, R. H. *Angew. Chem., Int. Ed.* **2000**, *39*, 3451−3453. Connon, S. J.; Blechert, S. *Angew. Chem., Int. Ed.* **2003**, *42*, 1900−1923. Schmidt, B. *Angew. Chem., Int. Ed.* **2003**, *42*, 4996−4999.

(16) Liu, X.; Guo, S.; Mirkin, C. A. *Angew. Chem., Int. Ed.* **2003**, *42*, 4785−4789. Li, X.-M.; Huskens, J.; Reinhoudt, D. N. *Nanotechnology* **2003**, *14*, 1064−1070. Harada, Y.; Girolami, G. S.; Nuzzo, R. G. *Langmuir* **2003**, *19*, 5104−5114. Rutenberg, I. M.; Scherman, O. A.; Grubbs, R. H.; Jiang, W.; Garfunkel, E.; Bao, Z. *J. Am. Chem. Soc.* **2004**, *126*, 4062−4063. Watson, K. J.; Zhu, J.; Nguyen, S. T.; Mirkin, C. A. *J. Am. Chem. Soc.* **1999**, *121*, 462−463. Jeon, N. L.; Choi, I. S.; Whitesides, G. M.; Kim, N. Y.; Laibinis, P. E.; Harada, Y.; Finnie, K. R.; Girolami, G. S.; Nuzzo, R. G. *Appl. Phys. Lett.* **1999**, *75*, 4201−4203. Weck, M.; Jackiw, J. J.; Rossi, R. R.; Weiss, P. S.; Grubbs, R. H. *J. Am. Chem. Soc.* **1999**, *121*, 4088−4089. Jordi, M. S.; Seery, T. A. P. *J. Am. Chem. Soc.* **2005**, *127*, 4416−4422. Gomez, F. J.; Chen, R. J.; Wang, D.; Waymouth, R. M.; Dai, H. *Chem. Commun.* **2003**, 190−191. Agnes, J.; Scherman, O. A.; Grubbs, R. H.; Lewis, N. S. *Langmuir* **2001**, *17*, 1321−1323. Kim, N. Y.; Jeon, N. L.; Choi, I. S.; Takami, S.; Harada, Y.; Finnie, K. R.; Girolami, G. S.; Nuzzo, R. G.; Whitesides, G. M.; Laibinis, P. E. *Macromolecules* **2000**, *33*, 2793−2795.

(17) Lee, J. K.; Lee, K.-B.; Kim, D. J.; Choi, I. S. *Langmuir* **2003**, *19*, 8141−8143.

refluxing chloroform for over 4 days.[12] These results are critical as they show that these monolayers are stable enough to have practical applications in fields such as biochemistry, sensors, and tribology. Although these monolayers are crystalline and stable under a variety of conditions, being terminated with methyl groups limits their use, especially with respect to further functionalization.

In this paper we report the assembly of mixed monolayers of 1-octadecene and $CH_2{=}CH(CH_2)_9O(CH_2)_9CH{=}CH_2$, **A** (Figure 1). We designed **A** as a suitable precursor to assemble monolayers as it is easy to synthesize in one step from commercially available starting materials and it assembles into monolayers that are thicker than those assembled from 1-octadecene. The latter point is important: a mixed monolayer of **A** and 1-octadecene will expose olefins on the monolayers above the methyl groups. Thus, the olefins will be easily accessible to react with the Grubbs' catalyst.

In this paper we will describe the straightforward, one-step synthesis of **A** and the assembly and characterization of mixed monolayers of **A** with 1-octadecene. These monolayers were characterized by X-ray photoelectron spectroscopy (XPS) and horizontal attenuated total reflection infrared spectroscopy (HATR-IR spectroscopy). In addition, we will describe our results for the functionalization of olefin-terminated monolayers with the Grubbs' first generation catalyst to yield monolayers terminated with acids, aldehydes, bromides, and alcohols. Finally, we will report mild methods to grow polymers from these monolayers and their patterning on the micrometer size scale.

Experimental Section

Materials and Methods. 1-Octadecene (90%), 10-undecenoic acid (98%), 10-undecen-1-ol (99%), 10-undecenal (97%), 11-bromo-1-undecene (95%), 1,6-dichlorohexane (95%), 1-undecanol (98%), potassium *tert*-butoxide, 5-norbornene-2-carboxylic acid (98%), and 48% hydrofluoric acid were purchased from Acros or Aldrich and used as received. 40% NH_4F was purchased from J. T. Baker and used as received. All solvents were purchased from Acros and used as received. Single-side polished Si(111) wafers (n-type) were purchased from Silicon Inc, Boise, ID.

TEMPO-C_{10} was synthesized as described in a previous paper.[11,12] It was stored in a −30 °C freezer in a glovebox under N_2. 1-Octadecene and 10-undecenoic acid were distilled with a Vigreux column under reduced pressure. Typically, 500 mL were distilled and the middle third of the fractional distillation was used. The collected fraction was transferred to a Kontes flask. The Kontes flask was evacuated under reduced pressure for 48 h and back-filled with N_2; this process was repeated three times. The Kontes flask was stored in the glovebox.

Instrumentation. ^{1}H and ^{13}C NMR were recorded on a Bruker DPX 300 using $CDCl_3$. The solvent signal was used as internal standard.

X-ray Photoelectron Spectroscopy (XPS). X-ray photoelectron spectra were obtained on a Kartos Axis Ultra Imaging spectrometer. Spectra of C(1s) (275−295 eV binding energy), O(1s) (525−545 eV binding energy), F(1s) (675−695 eV binding energy), Si(2p) (90−110 eV binding energy), Cl(2p) (190−210 eV binding energy), and Br(3d) (60−70 eV binding energy) as well as survey scans (0−1100 eV) were recorded with a tilt angle of 45°. The atomic compositions were corrected for atomic sensitivities and measured from high-resolution scans. The atomic sensitivities were 1.000 for F(1s), 0.780 for O(1s), 0.278 for C(1s), 0.328 for Si(2p), 0.891 for Cl(2p), and 1.055 for Br(3d).

Horizontal Attenuated Total Reflectance Infrared Spectroscopy. These spectra were recorded using a Bruker Tensor 27 equipped with an MCT detector cooled with liquid nitrogen. Monolayers were assembled on Si(111) HATR crystals with dimensions of 80 × 10 × 5 mm. The crystals were mounted in a dry air purged sample chamber. Background spectra were performed using freshly oxidized surfaces of HATR crystals. Scans were measured at a resolution of 4.0 or 2.0 cm^{-1}.

Scanning Electron Microscopy. Si(111) shards that were patterned as shown in Figure 12 were examined with a Hitachi S-4000 scanning electron microscope. Typically, an accelerating voltage of 5 kV was used to image the patterns on the surface.

Synthesis of 11,11′-Oxybis-1-undecene (A). 10-Undecen-1-ol (60 g, 0.352 mol), triethylamine (28.4 g, 0.281 mol), and *p*-tolulenesulfonyl chloride (26.8 g, 0.140 mol) were stirred under nitrogen at room temperature for 24 h in 360 mL of tetrahydrofuran (THF). Potassium *tert*-butoxide (39.4 g, 0.352 mol) was added to the reaction mixture and stirred for 7 h. The solvent was evaporated, and the product was extracted with methylene chloride. After evaporation the product was distilled as a colorless oil under vacuum at 200 °C and stored in a −30 °C freezer in a glovebox. Yield: 61%. ^{1}H NMR (300 MHz, $CDCl_3$, ppm): δ 5.82 (2H, m), 4.96 (4H, m), 3.38 (4H, t, $J = 6.9$ Hz), 2.02 (4H, q, $J = 6$ Hz), 1.54 (4H, m), 1.28 (24H, m). ^{13}C NMR (300 MHz, $CDCl_3$, ppm): δ 138.9, 114.0, 70.8, 33.7, 29.7, 29.4 (3 peaks), 29.0, 28.8, 26.1. HRMS. Calcd for $C_{22}H_{42}O$: 322.3236. Found: 322.3235.

Synthesis of $CH_2{=}CH(CH_2)_9O(CH_2)_{10}CH_3$. In a round-bottom flask, 1-undecanol (58.3 g, 0.154 mol) and potassium *tert*-butoxide (38.0 g, 0.339 mol) were added under nitrogen to 250 mL of THF. The solution turned yellow and cloudy. 11-Bromo-1-undecene (35.9 g, 0.154 mol) was added, and the mixture was refluxed under nitrogen. The product was isolated as a clear liquid by distillation under vacuum at 200 °C and stored in a −30 °C freezer in a glovebox. Yield: 44%. ^{1}H NMR (300 MHz, $CDCl_3$, ppm): δ 5.76 (1H, m), 4.92 (2H, m), 3.36 (4H, t, $J = 6$ Hz), 1.99 (2H, m), 1.52−1.25 (32H, m), 0.85 (3H, t, $J = 6$ Hz). ^{13}C NMR (300 MHz, $CDCl_3$, ppm): δ 139.2, 114.0, 70.9, 33.8, 31.9, 29.8, 29.6, 29.5, 29.4 (4 peaks), 29.3, 29.1, 28.9, 26.2, 22.7, 14.1. HRMS: Calcd for $C_{22}H_{44}O$: 324.3292. Found: 324.3291.

Synthesis of $CH_2{=}CH(CH_2)_9O(CH_2)_6Cl$. In a round-bottom flask, 10-undecen-1-ol (26.5 g, 0.156 mol) and potassium *tert*-butoxide (20.9 g, 0.339 mol) were added under nitrogen to 450 mL of THF. 1,6-Dichlorohexane (72.4 g, 0.467 mol) was added, and the mixture was refluxed under nitrogen. The solvent was removed by evaporation, and the product was extracted with methylene chloride from water. The product was purified by column chromatography with 3/97 ethyl acetate/hexane. Yield: 22%. ^{1}H NMR (300 MHz, $CDCl_3$, ppm): δ 5.79 (1H, m), 4.94 (2H, m), 3.46 (2H, t, $J = 6$ Hz), 3.34 (4H, m), 1.97 (2H, m), 1.71 (2H, m), 1.52−1.33 (20H, m). ^{13}C NMR (300 MHz, $CDCl_3$, ppm): δ 138.8, 113.9, 70.7, 70.4, 44.7, 33.6, 32.4, 29.6, 29.3 (4 peaks), 28.9, 28.7, 26.5, 26.0, 25.3. HRMS. Calcd for $C_{17}H_{33}ClO$: 288.2220. Found: 288.2216.

Assembly of Mixed Monolayers of 11,11′-Oxybis-1-undecene and 1-Octadecene. Silicon(111) shards cleaned with a nitrogen gun and rinsed with hexane, acetone, and methanol. The wafers were etched in 1:5 (v/v) of HF/NH_4F solution for 30 s. The wafers were oxidized with 1/3 (v/v) of H_2O_2/H_2SO_4 for 1 h at 90 °C. *Caution*: *Pirhana solution is highly dangerous and should be handled with care*. The oxidized wafers were washed with water. The wafers were then etched with 40% NH_4F for 30 min under an atmosphere of argon. This process yielded hydrogen-terminated silicon(111). The wafer was dried with a nitrogen gun and immediately transferred to a glovebox.

The shards were immersed in a solution of 11,11′-oxybis-1-undecene and 1-octadecene with 0.1 mol % of TEMPO-C_{10} in the glovebox. Typically, a mixed monolayer with a 1/1 mole ratio of 11,11′-oxybis-1-undecene/1-octadecene was assembled on the hydrogen-terminated Si(111) shards by mixing 11,11′-oxybis-1-undecene (3 mL, 2.3 g, 7.0 mmol) and 1-octadecene (2.34 mL, 1.84 g, 7.0 mmol) with 0.1 mol % of TEMPO-C_{10} (0.005 g, 0.007 mmol). The wafer was sealed in a Schlenk flask under nitrogen for 24 h. After 24 h, the shards were washed with various solvents and sonicated with CH_2Cl_2.

Representative Procedure for Cross-Metathesis on Mixed Monolayers. A Si(111) shard with an olefin-terminated monolayer, Grubbs' first generation catalyst (0.054 g, 0.06 mmol), CH_2Cl_2 (3 mL), and 10-undecenoic acid (1 mL, 5.4 mmol) were added to a

Table 1. XPS and HATR-IR Spectroscopy of Monolayers on Si(111)

		XPS composition[a] (%)				HATR-IR	
entry	composition[b]	C	Si	SiO_x	O	$\upsilon_a(CH_2)$ (cm^{-1})	$\upsilon_s(CH_2)$ (cm^{-1})
1	$CH_2{=}CH(CH_2)_{15}CH_3$	60	33	0	7.0	2920	2851
2	$CH_2{=}CH(CH_2)_9O(CH_2)_9CH{=}CH_2$	67	24	0	8.9	2925	2854
3	50/50 $CH_2{=}CH(CH_2)_{15}CH_3/CH_2{=}CH(CH_2)_9O(CH_2)_9CH{=}CH_2$	60	26	0	13	2924	2852
4	75/25 $CH_2{=}CH(CH_2)_{15}CH_3/CH_2{=}CH(CH_2)_9O(CH_2)_9CH{=}CH_2$	68	23	0	9	2924	2854
5	83/17 $CH_2{=}CH(CH_2)_{15}CH_3/CH_2{=}CH(CH_2)_9O(CH_2)_9CH{=}CH_2$	67	26	0	7	2923	2854
6	$CH_2{=}CH(CH_2)_9O(CH_2)_{10}CH_3$	c	c	c	c	2925	2854

[a] These compositions are from high-resolution scans. We studied the C(1s), Si(2p), and O(1s) peaks. The peak for SiO_x appeared at 102 eV in the Si(2p) high-resolution scan. [b] This column refers to the composition of reagents used to assemble the monolayers. All monolayers were assembled in the presence of 0.1 mol % TEMPO-C_{10}. For monolayers assembled from two components, we list the mole percent of each olefin that was used. [c] The XPS composition of this monolayer was not determined.

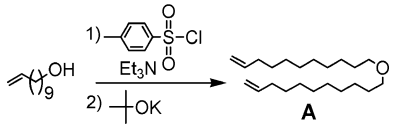

Figure 2. One-step synthesis of **A** from commercially available starting materials.

round-bottom flask in a glovebox. The flask was fitted with a reflux condenser and removed from the glovebox and attached to a nitrogen line. The reaction was refluxed under nitrogen for 48 h. The wafer was taken out and washed with hexanes, acetone, and methanol. The yield of the cross-metathesis reaction was determined by ^{1}H NMR. These conditions always gave a yield of 100%. ^{1}H NMR (300 MHz, $CDCl_3$, ppm): δ 5.36 (2H, br), 2.34 (4H, t, J = 6 Hz), 1.98 (4H, m), 1.60 (4H, m), 1.29 (20H, br).

Patterning Brush Polymers Using Soft Lithography. Typically, an olefin-terminated monolayer on a Si(111) shard was treated with a solution of Grubbs' first generation catalyst in methylene chloride for 30 min under ambient conditions. Next, the wafer was washed with methylene chloride and dried with nitrogen. A poly(dimethylsiloxane) (PDMS) stamp patterned in bas-relief was then pressed onto the surface, and a solution of 5-norbornene-2-carboxylic acid (0.01 g mL^{-1}) in dimethylformamide (DMF) was passed through the microchannels with a syringe pump for 1 h at the rate of 200 μL h^{-1}. The channels were then flushed with DMF for 1 h. The PDMS stamp was then removed and rotated at an angle, and the process was repeated. The wafer was washed with copious amounts of organic solvents and dried with nitrogen.

Results and Discussion

Assembly of Mixed Monolayers of 1-Octadecene and a Diolefin. We developed a simple, one-pot synthesis of **A** from commercially available starting materials (Figure 2). This method was used to synthesize up to 56 g of **A** that was readily cleaned by distillation. The full synthesis of **A** is described in the Experimental Section.

*Characterization of Monolayers of 1-Octadecene and **A***. Our method to assemble monolayers on Si(111) is shown in Figure 1. Higashi et al. reported a simple method to form hydrogen-terminated Si(111) with minimal defects (<1%).[9,10] Hydrogen-terminated Si(111) is air- and water-sensitive as it will readily oxidize to form a thin layer of silicon dioxide on the surface; however, well-ordered monolayers on Si(111) protect the surface from oxidation in air and solvents for days to months.[4,5,18] We used Higashi's method to form hydrogen-terminated Si(111) and then placed the wafer in mixtures of 1-octadecene, **A**, and TEMPO-C_{10}.

We characterized hydrogen-terminated Si(111) by horizontal attenuated total reflection infrared (HATR-IR) spectroscopy.[11] The Si(111)−H bonds are perpendicular to the surface and only IR-active with *p*-polarized light and are not seen with *s*-polarized light. Higashi et al. reported that the Si(111)−H peak appears at 2083.7 cm^{-1} with a narrow full width at half-maximum (fwhm) of 0.95 cm^{-1}.[10] Our hydrogen-terminated Si(111) surfaces are well-ordered as we observed one peak with *p*-polarized light at 2084 cm^{-1} with a fwhm of 3.8 cm^{-1} and no peaks with *s*-polarized light. Our results demonstrated that we formed a well-ordered hydrogen-terminated Si(111) surface.

To fully characterize monolayers, multiple methods must be used. We characterized our monolayers by XPS and HATR-IR spectroscopy. From our previous work on the assembly of monolayers of 1-octadecene with TEMPO, we learned several important characteristics of these monolayers that are important for the interpretation of the characterization of the monolayers reported in this paper.[11,12] First, we know that this method results in the assembly of a monolayer with a thickness given by ellipsometry of approximately 1.8 nm. Second, the monolayer is almost entirely composed of 1-octadecene with less than 1 mol % of TEMPO on the surface. Third, although TEMPO is necessary for the assembly of a well-ordered monolayer, we do not know the mechanism of assembly or the role of TEMPO.

In Table 1 and Figure 3 we show the XPS spectra of monolayers assembled from **A**. This surface was first characterized by a survey scan that showed the presence of Si, C, and O and high-resolution scans of Si, C, O, and F. The region for F was examined as hydrogen-terminated Si(111) was formed in 40% H_4NF, and we wished to look for the presence of Si−F or C−F bonds. The silicon region was interesting for what it did not show; we did not observe evidence for SiO_x. The bulk Si peak appears approximately 4 eV lower than the peak for SiO_x, and these peaks are thus easily separated and analyzed. We looked for SiO_x since unlike disordered monolayers, well-ordered monolayers protect silicon from oxidation. The XPS samples were allowed to sit exposed to atmospheric conditions for 2−4 weeks prior to their characterization by XPS. If the monolayers were disordered, the silicon surfaces would have oxidized during this time period. The lack of SiO_x in the XPS spectra indicates that well-ordered monolayers were assembled. The presence of a broad peak for O was consistent with our previous results for monolayers assembled from TEMPO-C_{10} and 1-octadecene. As there are many sources for oxygen including the ether oxygen in **A**, the three oxygens in TEMPO-C_{10}, and SiO_x we cannot make further assignments to this peak.

The C(1s) peak in the XPS spectra of monolayers assembled from 1-octadecene or **A** showed the presence of a Si−C bond and described the thickness of these monolayers. In a recent publication detailing the XPS characterization of organic monolayers on Si(111), Allongue et al. described the presence of a Si−C peak at binding energies approximately 0.9 eV lower

(18) Cicero, R. L.; Linford, M. R.; Chidsey, C. E. D. *Langmuir* **2000**, *16*, 5688−5695.

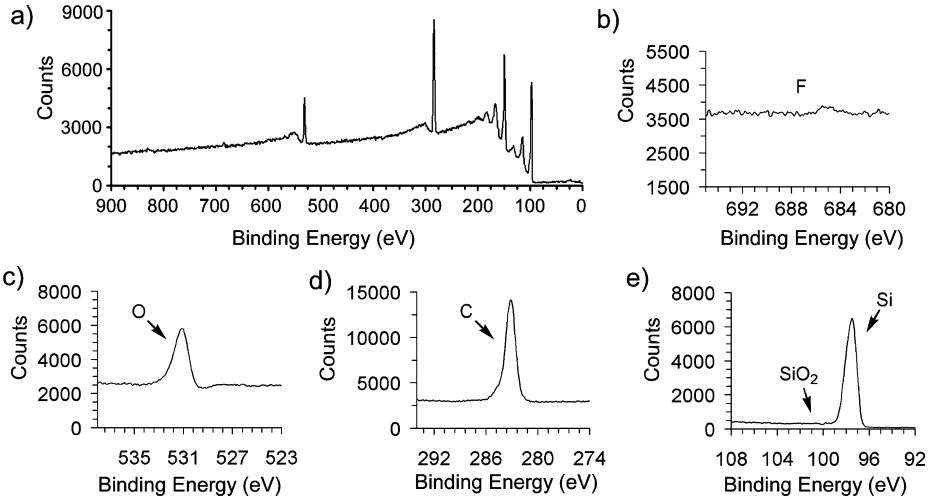

Figure 3. XPS of monolayers assembled from **A**. (a) A survey scan of this monolayer described the presence of C, O, and Si. High-resolution scans of (b) F(1s), (c) O(1s), (d) C(1s), and (e) Si(2p) were obtained to find the compositions of these monolayers as described in Table 1.

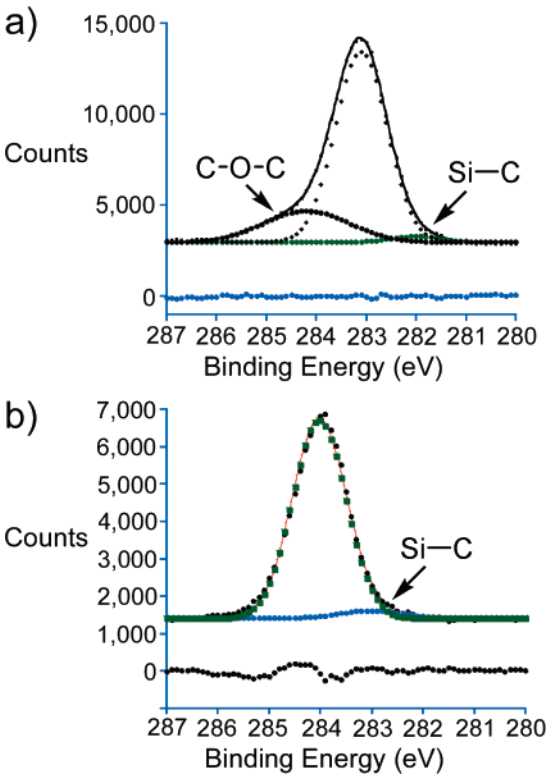

Figure 4. XPS of the C(1s) region of a monolayer assembled from (a) **A** and (b) 1-octadecene. Each of these monolayers was assembled with 0.1 mol % TEMPO-C_{10}. We fit the peak in a to three peaks and the peak in b to two peaks. The residuals to the fits are shown beneath each peak.

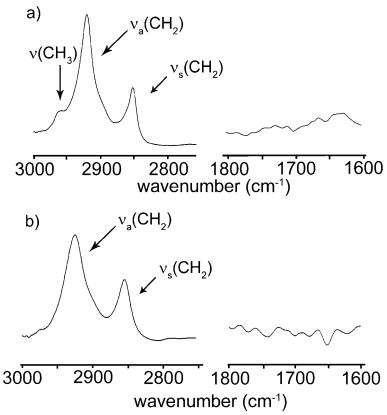

Figure 5. HATR-IR spectrographs of monolayers assembled from 0.1 mol % TEMPO-C_{10} and (a) 1-octadecene and (b) **A**. We did not observe an olefin peak at in the spectrum of monolayers composed of A.

than the main C−C peak.[19] They outlined how to use the integration of that peak relative to the integration of all carbon in the XPS to find a thickness for the monolayer. We fit the carbon peaks from monolayers assembled from 1-octadecene (Figure 4b) or **A** (Figure 4a) using the values from Allongue et al. and found the presence of Si−C bonds. The Si−C peak from monolayers assembled only from 1-octadecene integrated to 4.1% of the total amount of carbon. This value gave a thickness for the monolayer of 20 Å which matches the predicted value for the monolayer and agreed well with the previously measured ellipsometric thickness of 18 Å.[12]

The C(1s) region in the XPS of monolayers assembled from **A** fit to three different peaks. The largest peak was assigned to the majority of the carbons on the monolayer. A smaller peak at a binding energy of 1.2 eV higher than the largest peak was assigned to the carbons next to the oxygen in **A**. This peak was not present in monolayers assembled from 1-octadecene as that molecule lacks an ether bond. Finally, a small peak at a binding energy 0.7 eV lower than the main carbon peak was assigned to carbon bonded to silicon. This peak integrated to 2.7% of the total amount of carbon. Using the method of Allongue et al., this integration yielded a monolayer thickness of 25 Å.[19] This value agrees with the predicted thickness of 25.2 Å for these monolayers with a tilt angle of 35.5° and provides further evidence that an ordered monolayer was assembled through one olefin on **A**. Monolayers assembled through both olefins would have thicknesses of less than half of that value.

The HATR-IR spectrum of a monolayer of 1-octadecene shows two important peaks (Figure 5). The peaks corresponding to the antisymmetric—$\upsilon_a(CH_2)$—and symmetric—$\upsilon_s(CH_2)$—stretches for methylene appear at 2920 and 2851 cm^{-1}. These results are significant as the $\upsilon_a(CH_2)$ peak for crystalline monolayers ranges from 2918 to 2920 cm^{-1}, but for disordered monolayers it ranges

(19) Wallart, X.; de Villeneuve, C. H.; Allongue, P. *J. Am. Chem. Soc.* **2005**, *127*, 7871−7878.

Table 2. Different Reaction Conditions To Optimize the Cross Metathesis of 11-Undecylenic Acid As Shown in Figure 6

amount of olefin[a] (mL)	solvent	amount of solvent (mL)	Grubbs' catalyst[b] (mol %)	temp (°C)	vacuum	time (h)	yield[c] (%)
1.36	xylenes	4.5	0.32	25	no	22	16
1.28	xylenes	4.5	0.32	40	no	21	23
1.0	xylenes	3.0	1.0	40	no	41	47
1.0	xylenes	3.0	1.0	55	no	30	58
1.0	xylenes	3.0	1.0	70	no	50	91
1.0	xylenes	3.0	1.0	85	no	72	91
4.3	none		0.32	40	no	20	59
1.0	tetrakis(ethylene glycol)	3.0	1.0	25	yes	46	54
1.0	tetrakis(ethylene glycol)	3.0	1.0	40	yes	19	69
1.0	poly(ethylene glycol), 600 M_w	3.0	1.0	60	yes	113	72
1.0	silicon oil	3.0	1.0	40	yes	48	73
1.0	methylene chloride	3.0	1.0	reflux	no	48	100

[a] Each of these reactions was carried out under an atmosphere of N_2 or under vacuum (approximately 100 mTorr). [b] The mole percent of catalyst relative to undecylenic acid. [c] The yield refers to undecylenic acid that was cross metathesized to $=(CH(CH_2)_8CO_2H)_2$.

from 2925 to 2928 cm^{-1}.[4,20] Similarly, the $\upsilon_s(CH_2)$ peak for crystalline monolayers appears at 2850 cm^{-1}, but for disordered monolayers it appears at 2858 cm^{-1}.[4,20] The location of $\upsilon_a(CH_2)$ and $\upsilon_s(CH_2)$ peaks within these ranges describes the crystallinity of monolayers. Our results indicate that we assembled crystalline monolayers.

Monolayers assembled from **A** had peaks for $\upsilon_a(CH_2)$ and $\upsilon_s(CH_2)$ at 2925 and 2954 cm^{-1} (Table 1 and Figure 5). This result was surprising as results from XPS indicated that well-ordered monolayers were assembled but results from HATR-IR spectra indicated that the monolayers were disordered. To further investigate this discrepancy, we assembled mixed monolayers of **A** and 1-octadecene. As we increased the ratio of 1-octadecene to **A** in solutions used for the assembly, the values for $\upsilon_a(CH_2)$ and $\upsilon_s(CH_2)$ decreased and indicated that mixed monolayers were more ordered than those assembled only from **A** (Table 1, entries 2−5). We also did not observe a peak for the olefin at approximately 1641 cm^{-1}. This peak is typically weak and difficult to observe; it also may have packed on the surface such that it was not IR-active.[21,22] Although we did not see the olefin by HATR-IR spectroscopy, it was present; in the following sections we will describe how these monolayers reacted by cross metathesis and ring opening metathesis polymerizations from the olefins on the surface.

The two major differences between **A** and 1-octadecene are the presence of an ether and second olefin in **A**. From the literature of monolayers on gold we know several important characteristics about how molecules with these functional groups assemble into monolayers.[23,24] Ether bonds promote disorder in monolayers as they favor gauche over trans conformations by approximately 0.1−0.2 kcal mol^{-1}.[25] Whitesides et al. studied monolayers on gold assembled from thiols containing ether bonds by IR spectroscopy and observed several unresolved components near the $\upsilon_a(CH_2)$ and $\upsilon_s(CH_2)$ peaks.[24,25] This work indicated, but did not prove, that the monolayer was not a homogeneous distribution of methylenes. Ether bonds are well-known to affect the vibrational frequencies of methylenes and that this effect will

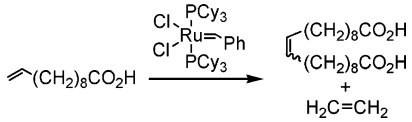

Figure 6. Reaction conditions of this cross metathesis reaction were optimized to yield a quantitative yield of product.

increase as the tilt angle of the monolayer increases. These effects place shoulders at slightly higher vibrational frequencies for the $\upsilon_a(CH_2)$ and $\upsilon_s(CH_2)$ peaks of a crystalline hydrocarbon and, if the shoulders were not resolved from the $\upsilon_a(CH_2)$ and $\upsilon_s(CH_2)$ peaks, would cause the $\upsilon_a(CH_2)$ and $\upsilon_s(CH_2)$ peaks to appear to shift to higher frequencies. This is important as we did not observe shoulders on the $\upsilon_a(CH_2)$ and $\upsilon_s(CH_2)$ peaks in our spectra as expected. Thus, our reported values for $\upsilon_a(CH_2)$ and $\upsilon_s(CH_2)$ may not be the true values for these peaks.

In contrast, the presence of a terminal olefin on monolayers of $HS(CH_2)_9CH{=}CH_2$ on gold do not cause these monolayers to appear disordered.[17,22] From this we know that monolayers terminated with olefins can pack into an all-trans, crystalline conformation. Of course it is important to note that monolayers on gold assemble through thiols, whereas monolayers on silicon assemble through olefins. Thus, the interpretation of the HATR-IR of a diolefin such as **A** is more complicated as it may bond twice to silicon through both olefins and assemble into a disordered monolayer.

We synthesized $CH_2{=}CH(CH_2)_9O(CH_2)_{10}CH_3$ (**B**) to study how the presence of an ether affects the $\upsilon_a(CH_2)$ and $\upsilon_s(CH_2)$ peaks for monolayers on silicon. Monolayers assembled from **B** in 0.1 mol % TEMPO-C_{10} appeared disordered by HATR-IR spectroscopy (Table 1, entry 6). This result was surprising and indicated that one internal ether bond or a second olefin may affect the order of a monolayer on silicon. We are not surprised that a second olefin may introduce some disorder as it may bond to the surface twice and increase the disorder, but we expected that monolayers assembled from **B** would appear ordered. It is surprising that one ether bond would have such an impact on monolayers on Si(111), and this work suggests that the structure of monolayers containing ether bonds or olefins deserve a full study that is beyond the scope of this paper.

Because of the limitations of HATR-IR spectroscopy, we were unable to determine if monolayers assembled from **A** were ordered or disordered. Our peaks were broad, and we were unable to distinguish the presence of shoulders on the $\upsilon_a(CH_2)$ and $\upsilon_s(CH_2)$ peaks, although Whitesides et al. described their presence on monolayers on Au. XPS data are consistent with an ordered monolayer, but HATR-IR data are consistent with a disordered monolayer.

(20) Porter, M. D.; Bright, T. B.; Allara, D. L.; Chidsey, C. E. D. *J. Am. Chem. Soc.* **1987**, *109*, 3559−3568. Snyder, R. G.; Strauss, H. L.; Elliger, C. A. *J. Phys. Chem.* **1982**, *86*, 5145−5150.

(21) Dubowski, Y.; Vieceli, J.; Tobias, D. J.; Gomez, A.; Lin, A.; Nizkoorodor, S. A.; Mcintire, T. M.; Finlayson-Pitts, B. J. *J. Phys. Chem. A* **2004**, *108*, 10473−10485.

(22) Peanasky, J. S.; McCarley, R. L. *Langmuir* **1998**, *14*, 113−123.

(23) Wenzel, I.; Yam, C. M.; Barriet, D.; Lee, T. R. *Langmuir* **2003**, *119*, 10217−10224. Sinniah, K.; Cheng, J.; Terrettaz, S.; Reutt-Robey, J. E.; Miller, C. J. *J. Phys. Chem.* **1995**, *99*, 14500−14505.

(24) Laibinis, P. E.; Bain, C. D.; Nuzzo, R. G.; Whitesides, G. M. *J. Phys. Chem.* **1995**, *99*, 7663−7676.

(25) Miwa, Y.; Machida, K. *J. Am. Chem. Soc.* **1989**, *111*, 7733−7739.

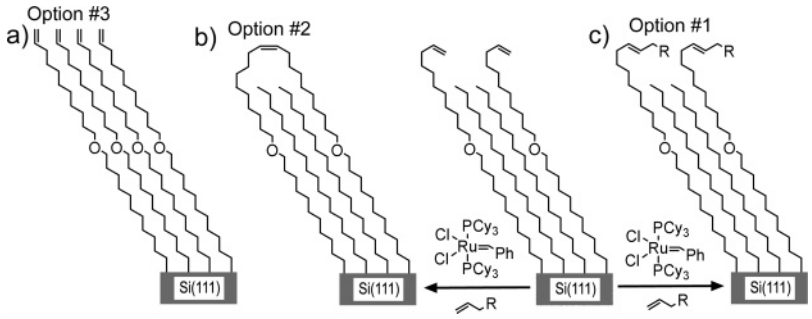

Figure 7. Three possible outcomes for the reaction of monolayers of **A** and 1-octadecene with the Grubbs' catalyst and an olefin in solution. (a) Areas with well-ordered monolayers of **A** may be too sterically hindered to allow the Grubbs' catalyst to react. (b) Olefins on the monolayer may react with each other or (c) with an olefin in solution.

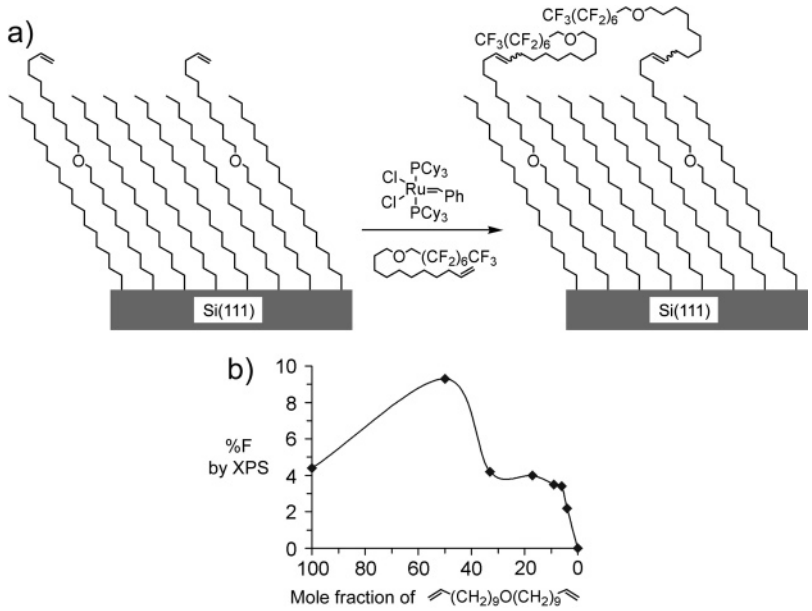

Figure 8. (a) Olefin-terminated monolayers reacted with an olefin in solution with 15 fluorines to yield fluorinated surfaces. These surfaces were studied by XPS to describe the relative amounts of fluorine on the monolayers. (b) Amount of fluorine on these surfaces as a function of the mole fraction of **A** used in the assembly of the monolayer. The line is drawn as a guide to the reader and is not fitted from an equation.

Cross Metathesis on Olefin-Terminated SAMs. We first explored a simple cross metathesis reaction between two molecules of undecylenic acid to learn which conditions are needed to push the reaction to completion (Figure 6). These reactions were stopped after a period of time, the solvent was removed, and the yield was studied by ^{1}H NMR spectroscopy. Hydrogens on the starting olefin appeared at 5.0 and 5.8 ppm, and those on the product appeared at 5.4 ppm; the yield was simple to determine on the basis of this information. We choose to use undecylenic acid for our test reaction as it has a high boiling point that limited its loss under vacuum (boiling point of 137 °C at 2 mm of Hg) and a carboxylic acid. Monolayers functionalized with carboxylic acids are important as they can be readily reacted to expose more complex molecules.

The reaction conditions that we tried are shown in Table 2. Initial attempts in xylene, silicon oil, tetrakis(ethylene glycol), and poly(ethylene glycol) were not successful due to poor catalyst solubility. Heating these reactions to speed the reaction or placing them under vacuum to remove ethylene increased the yield but were ultimately unsuccessful. Refluxing methylene chloride was attempted as the catalyst was soluble in this solvent and refluxing helped remove ethylene from the reaction mixture to drive the reaction forward. The yield of this reaction was >97% by ^{1}H NMR and worked for all olefins that we attempted.

Cross Metathesis between Olefin-Terminated Monolayers and Fluorinated Olefins. Although we found reaction conditions that allow for low catalyst loadings and quantitative cross metathesis reactions, it is important to note that these conditions were for olefins in solution rather than those on monolayers. Olefins exposed on a monolayer may undergo three different reactions when reacted with the Grubbs' catalyst in the presence of an olefin in solution (Figure 7). First, olefin-terminated monolayers may react with olefins in solution and yield functionalized surfaces (option no. 1 in Figure 7). Second, olefins on the monolayer may undergo cross metathesis with each other (option no. 2 in Figure 7). Third, olefins on the monolayer may be too sterically hindered from reacting with the Grubbs' catalyst (option no. 3 in Figure 7). These three possible outcomes complicate our interpretation of olefin-terminated monolayers that reacted with the Grubbs' catalyst and an olefin in solution.

To study the yield of cross metathesis on olefins exposed on a monolayer, we synthesized $CH_2{=}CH(CH_2)_9OCH_2(CF_2)_6CF_3$ (Figure 8). The fluorines on this molecule gave us a unique handle in the XPS that we could use to study cross metathesis on monolayers. We first assembled monolayers on silicon from different ratios of **A** and 1-octadecene. Next, we reacted these monolayers with the Grubbs' catalyst and $CH_2{=}CH(CH_2)_9$-$OCH_2(CF_2)_6CF_3$ in refluxing methylene chloride. Finally, these surfaces were studied by XPS for C, F, Si, and O. The results are shown in Figure 8b.

These experiments showed that the highest concentration of fluorine on the surface was observed for monolayers assembled

Table 3. Cross Metathesis between Olefin-Terminated Monolayers and Functional Olefins in Solution

		XPS composition (%)					HATR-I R spectroscopy		
entry	olefin	C	Si	SiO_x	F	O	$\upsilon_a(CH_2)$ (cm^{-1})	$\upsilon_s(CH_2)$ (cm^{-1})	$\nu(C{=}O)$ (cm^{-1})
1	$CH_2{=}CH(CH_2)_8CO_2H$	58	22	0	0	20	2924	2854	1739, 1700
2	$CH_2{=}CH(CH_2)_9OH$	67	23	0	0	10	2925	2855	1739[a]
3	$CH_2{=}CH(CH_2)_8CHO$	68	19	0	0	12	2925	2854	1730

[a] After cross metathesis with the monolayer, the alcohol was reacted with acetyl chloride. We report the carbonyl peaks of the ester.

from 50% **A** and 50% 1-octadecene. Interestingly, monolayers assembled only from **A** had a lower amount of fluorine on the surface. This result suggests that either cross metathesis between olefins on the monolayer was significant or that the monolayers were too ordered to fully react with the Grubbs' catalyst. For surfaces with decreasing mole fractions of **A** used in their assembly, the amount of fluorine observed by XPS slowly decreased. The shape of the curve in Figure 8 is complex due to the three possible reactions outlined in Figure 7, steric crowding of olefins on the surface that have reacted and block the Grubbs' catalyst from unreacted olefins on the surface, and different packing of monolayers after cross metathesis. Despite the limitations in fully characterizing the shape of the curve, it clearly describes how to optimize the concentration of reacted olefins on the monolayer.

These experiments also clearly demonstrated that monolayers assembled from $CH_2{=}CH(CH_2)_9O(CH_2)_9CH{=}CH_2$ exposed olefins on the surface that were reactive with the Grubbs' catalyst. Monolayers assembled from 1-octadecene that did not display olefins were not reactive with the Grubbs' catalyst. These monolayers did not show any fluorine in the XPS after reaction with the Grubbs' catalyst and $CH_2{=}CH(CH_2)_9OCH_2(CF_2)_6CF_3$ (Figure 8).

We estimated the yield of cross metathesis between olefins on the surface and those in solution for a monolayer assembled from a 1/1 mole ratio of **A** to 1-octadecene after making several reasonable assumptions.[19,26] We first assumed that the ratio of **A** to 1-octadecene in solution will match the ratio on the surface—this assumption will be supported by experimental evidence in the following section. Next, we assumed that the monolayer was well-packed and that the fluorinated alkane was found on the top. We used 35.4 Å for the attenuation length of electrons through the monolayer and estimated the ratio of F to C if all of the surface olefins reacted with olefins in solution.[19] With these assumptions, the value for F/C was 0.30 which is twice the observed value of 0.15. This estimate indicates that approximately half of the olefins on the surface reacted with olefins in solution; the remaining olefins either reacted by cross metathesis with another olefin on the surface or remain unreacted. Although this estimate for the "yield" encompasses several approximations, it provides a description for how many surface-bound olefins react with olefins in solution for a monolayer assembled from a 1/1 mole ratio of **A** to 1-octadecene.

We studied these surfaces by HATR-IR spectroscopy but could not distinguish between the three different outcomes shown in Figure 7. Due to strong absorptions below 1500 cm^{-1}, HATR-IR spectroscopy on Si(111) shards cannot image peaks below this cutoff, and the peaks in the C−H region were too broad to distinguish the different olefins that may be present on the surface. Nevertheless, these results are important as we learned how to optimize the ratio of **A** to 1-octadecene in solution to functionalize surfaces.

Composition of Mixed Monolayers. We do not know how the ratio of **A** to 1-octadecene used in the assembly of monolayers relates to their final composition. For instance, we do not know if a 1/1 molar ratio of **A** to 1-octadecene in solution results in a 1/1 ratio of these molecules in the monolayer. The studies that we discussed previously cannot describe the composition on the surface due to potential cross metathesis between olefins on the monolayers and incomplete cross metathesis between olefins in solution with those on the surface. We needed a cleaner system to study the composition of monolayers assembled from two different molecules.

To learn how the composition of solutions used in the assembly relates to the final composition of monolayers, we synthesized $CH_2{=}CH(CH_2)_9O(CH_2)_6Cl$. Monolayers assembled from this molecule will have the same thickness as a monolayer assembled from 1-octadecene and expose a chlorine on the top of the monolayer. By measuring the ratio of chlorine to carbon by XPS for monolayers assembled from mixtures of $CH_2{=}CH(CH_2)_9O(CH_2)_6Cl$ and 1-octadecene, we can learn the composition of these monolayers. Our results in Figure 9 demonstrate that the

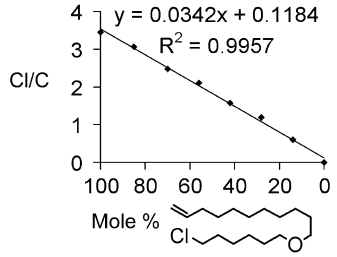

Figure 9. Ratio of the areas of the Cl(2p) and C(1s) peaks from the XPS of monolayers assembled from $CH_2{=}CH(CH_2)_9O(CH_2)_6Cl$ and 1-octadecene. The *x*-axis shows the mole percent of $CH_2{=}CH(CH_2)_9O(CH_2)_6Cl$ used in the assembly of the monolayers.

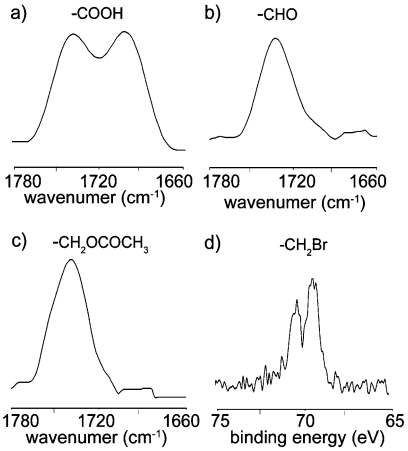

Figure 10. HATR-IR spectrographs of the carbonyl regions for monolayers reacted with (a) $CH_2{=}CH(CH_2)_8CO_2H$, (b) $CH_2{=}CH(CH_2)_8CHO$, and (c) $CH_2{=}CH(CH_2)_9OH$. The alcohols on monolayers that were reacted with $CH_2{=}CH(CH_2)_9OH$ were further functionalized with $ClCOCH_3$ to yield ester-terminated monolayers which were characterized by HATR-IR spectroscopy. These spectrographs show the presence of carbonyl peaks. (d) High-resolution XPS of the Br(3d) region for an olefin-terminated monolayer after reaction with $CH_2{=}CH(CH_2)_9Br$. This XPS shows the presence of Br on the surface.

(26) Lamont, C. L. A.; Wilkes, J. *Langmuir* **1999**, *15*, 2037−2042. Laibinis, P. E.; Bain, C. D.; Whitesides, G. M. *J. Phys. Chem.* **1991**, *95*, 7017−7021.

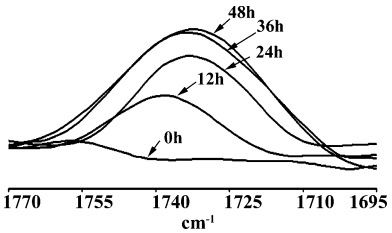

Figure 11. Carbonyl peak at different reaction times for cross metathesis between an olefin-terminated monolayer and $CH_2{=}CH(CH_2)_8COH$. The carbonyl peak rapidly grew in intensity but did not appreciably change after 36 h, indicating that the reaction was complete.

ratio of $CH_2{=}CH(CH_2)_9O(CH_2)_6Cl$ to 1-octadecene in solution closely follows the ratio of these molecules in the monolayer.

Cross Metathesis with Olefins Exposing Useful Functional Groups. Since the Grubbs' catalyst is stable in the presence of many functional groups, monolayers displaying a variety of different functional groups can be synthesized. To demonstrate this potential, we reacted monolayers assembled from 50% **A** and 50% 1-octadecene with olefins terminated with alcohols, bromides, aldehydes, and carboxylic acids. We studied these surfaces by XPS and HATR-IR spectroscopy (Table 3 and Figure 10). These results indicated that each monolayer was functionalized with an olefin and exposed different functional groups on the surface.

Kinetics of Reaction of Olefin-Terminated Monolayers with $CH_2{=}CH(CH_2)_8COH$. We wished to probe how quickly the surface was functionalized by reaction with the Grubbs' catalyst. All of our cross metathesis reactions were run for 48 h on the basis of analogy with the solution-phase reaction that is complete after this time. Because surface reactions can show much different kinetics than those in solution, we decided to follow the reaction of $CH_2{=}CH(CH_2)_8COH$ with an olefin-terminated monolayer as a function of time (Figure 11). Specifically, we studied the carbonyl peak as it appeared separated from other peaks and had a strong intensity. We assembled mixed monolayers from a 1/2 molar ratio of $CH_2{=}CH(CH_2)_9O(CH_2)_9CH{=}CH_2$/1-octadecene on several silicon shards and subjected them to the cross metathesis conditions for 6, 12, 24, 36, and 48 h. The shards were rinsed and studied by HATR-IR spectroscopy. The results of these experiments show that the carbonyl peak grew in rapidly within 24 h and did not increase from 36 to 48 h (Figure 11). This demonstrated that the reaction between olefins on the surface and olefins in solution was complete within 48 h.

Patterning Monolayers on the Micrometer Size-Scale Using Soft Lithography. In this section we will report methods to pattern these monolayers on the micrometer-size scale by soft lithography. Specifically, we patterned PDMS on the micrometer-size scale such that a series of microchannels were formed when a PDMS stamp was placed against a silicon wafer. These microchannels were easily accessible by an external syringe pump to add reagents only to the microchannels. Monolayers in contact with PDMS were protected from reaction. We chose soft lithography as these techniques have become well accepted in the scientific community, they are used to pattern monolayers on gold, and their applications to form microfluidic channels are becoming increasingly important.[27] Generating patterns by soft lithography is rapid as PDMS stamps are readily manufactured in under 24 h.[28]

Our general method is outlined in Figure 12. To demonstrate this method, we patterned monolayers through cross metathesis

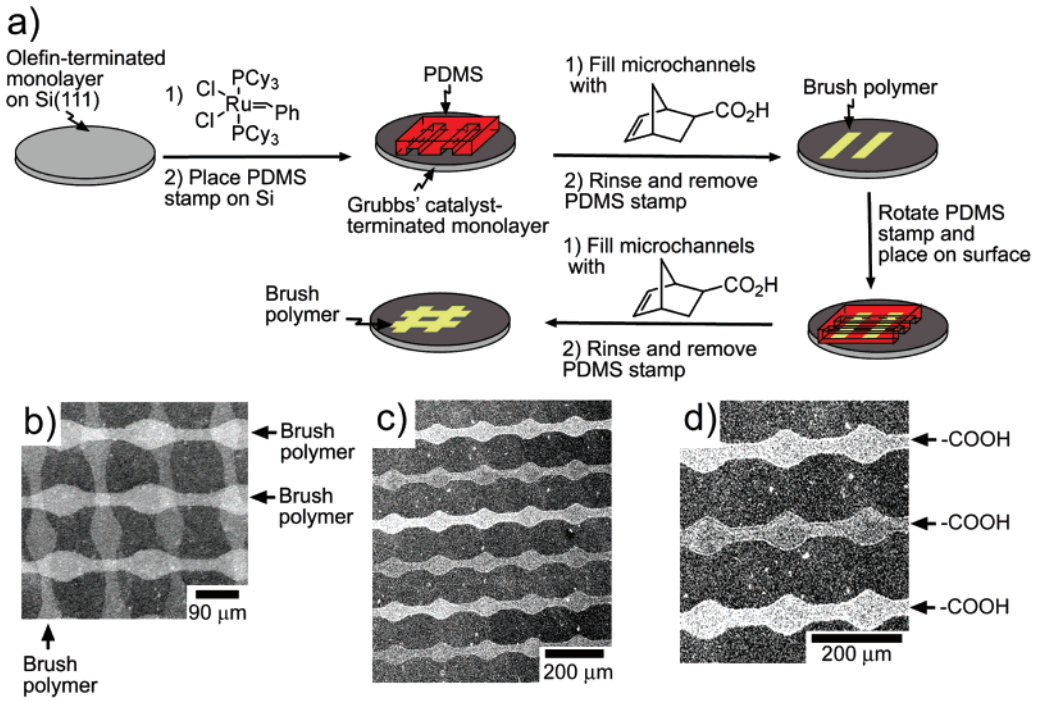

Figure 12. (a) Method for patterning olefin-terminated monolayers on Si(111) with the Grubbs' catalyst. First, we assembled a mixed monolayer of **A** and 1-octadecene. Next, we immersed the silicon wafer in a solution of the Grubbs' first generation catalyst for 15 min. The Grubbs' catalyst attached to the monolayer by cross metathesis with an olefin on the surface. A PDMS stamp was then placed on the monolayer to form microfluidic channels on the surface. Next, a solution of an olefin filled the channels by an external syringe (not shown). Monolayers in contact with PDMS were not exposed to the olefins and did not react. After 15−30 min, the channels were rinsed and the PDMS stamp was removed and turned 90° before being placed on the monolayer again. A new solution of an olefin added to the channels. Finally, the channels were rinsed, the PDMS stamp was removed, and the silicon wafer was rinsed. (b) SEM micrograph of crossed brush polymers synthesized as in part a. (c and d) SEM micrographs of monolayers reacted by cross metathesis with $CH_2{=}CH(CH_2)_8CO_2H$ to expose acids along the surface. In these experiments $CH_2{=}CH(CH_2)_8CO_2H$ was added to the microchannels rather than 5-norbornene-2-carboxylic acid. The image in d is a close-up of the image in c.

and ring opening polymerizations (ROMP). In a one example we chose to grow polymer brushes from the surfaces using ROMP as the Grubbs' catalyst polymerizes strained monomers under living conditions. We chose to synthesize polymer brushes of 5-norbornene-2-carboxylic acid because it polymerizes rapidly and exposes carboxylic acids on the surface (Figure 12b). These polymer brushes were covalently attached to the surface and could not be washed from the surface. In a second example we patterned monolayers by cross metathesis using solutions of $CH_2{=}CH(CH_2)_8CO_2H$ (Figure 12c,d). These methods demonstrate that we can pattern monolayers using either cross metathesis or ROMP.

Conclusions

The main accomplishments of this work are the assembly and characterization of monolayers of **A**, the cross metathesis of olefin-terminated monolayers on Si(111), and the patterning of these monolayers using ROMP and cross metathesis. We patterned surfaces that exposed alkyl bromides, aldehydes, carboxylic acids, and alcohols and demonstrated how these surfaces may be patterned. These functional groups are important as we and others reported methods to further functionalize them to expose DNA, proteins, and other important molecules. Thus, the method we report in this paper is applicable to the complex functionalization of monolayers on silicon.

This work may have applications in a variety of areas that employ monolayers on silicon. Efforts to selectively functionalize its surface by organic chemistry are critical for applications in biotechnology and nanotechnology, such as biosensors and nanoelectronic chips that exploit the unique electronic properties of silicon. Our simple synthetic route to **A** facilitates use of the patterning methodology reported here also by researchers that are not skilled in organic synthesis. In addition, the ability to pattern these monolayers on silicon with a wide variety of end groups using soft lithography, i.e., microfluidic patterning and microcontact printing, further expands their applicability to cases where localized tailoring of physical and chemical surface properties is desired.

Acknowledgment. We thank the University of Iowa, MPSF Program, Carver Scientific Research Initiative Grants Program, and the donors of the ACS Petroleum Research Fund for funding. This work was partly carried out in the Center for Microanalysis of Materials, University of Illinois, which is partially supported by the U.S. Department of Energy under Grant DEFG02-91-ER45439. We gratefully thank Rick Haasch for many helpful discussions and help with the XPS. We thank Jonas Baltrusaitis for help with Figure 10d.

Supporting Information Available: ^{1}H NMR spectra of $CH_2{=}CH(CH_2)_9O(CH_2)_9CH{=}CH_2$, $CH_2{=}CH(CH_2)_9O(CH_2)_{10}CH_3$, and $CH_2{=}CH(CH_2)_9O(CH_2)_6Cl$ (PDF). This material is available free of charge via the Internet at http://pubs.acs.org.

LA0532196

(27) Aizenberg, J. *Adv. Mater.* **2004**, *16*, 1295−1302. Bruinink, C. M.; Peter, M.; de Boer, M.; Kuipers, L.; Huskens, J.; Reinhoudt, D. N. *Adv. Mater.* **2004**, *16*, 1086−1090. Kane, R. S.; Stroock, A. D.; Jeon, N. L.; Ingber, D. E.; Whitesides, G. M. *Opt. Biosens.* **2002**, 571−595. Kane, R. S.; Takayama, S.; Ostuni, E.; Ingber, D. E.; Whitesides, G. M. *Biomaterials* **1999**, *20*, 2363−2376. Lee, C. J.; Blumenkranz, M. S.; Fishman, H. A.; Bent, S. F. *Langmuir* **2004**, *20*, 4155−4161. McDonald, J. C.; Duffy, D. C.; Anderson, J. R.; Chiu, D. T.; Wu, H.; Schueller, O. J.; Whitesides, G. M. *Electrophoresis* **2000**, *21*, 27−40. Rolland, J.; Hagberg, E. C.; Dension, G. M.; Carter, K. R.; De Simone, J. M. *Angew. Chem., Int. Ed.* **2004**, *43*, 5796−5799. Whitesides, G. M.; Ostuni, E.; Takayama, S.; Jiang, X.; Ingber, D. E. *Annu. Rev. Biomed. Eng.* **2001**, *3*, 335−373. Xia, Y.; Whitesides, G. M. *Angew. Chem., Int. Ed.* **1998**, *37*, 550−575.

(28) Qin, D.; Xia, Y.; Whitesides, G. M. *Adv. Mater.* **1996**, *8*, 917−919.